

Structure and vibration characteristics of Ti-Al-Mo-V alloy

FEI-YI HUNG*, TRUAN-SHENG LUI

Department of Materials Science and Engineering, National Cheng Kung University, Tainan, Taiwan 701, Republic of China

E-mail: fyhung@mail.mse.ncku.edu.tw

Ti-5Al-2.5Mo-1.4V rolled plates were subjected to solid-solution heat treatment at 870 or 930°C for 1 h and aged for 1–8 h at 460°C to investigate the relationship between the microstructure and the vibration characteristics of the alloy. According to the experimental results, the S870 solid solution matrix contains $\alpha + \alpha' + \beta$ structures and the S930 solid solution specimen possesses $\alpha + \alpha'$ structures (β transus is $\sim 900^\circ\text{C}$). Increasing the α' phase content improves strength and hardness but reduces ductility. It also promotes internal friction and thus increases damping. During the 460°C aging process, the α' phase in the β region of S870/Ah grows and transforms into a finer needle structure and the primary α phase (bounded by prior β grain boundary) of S930/Ah grows within the α' matrix. Both S830/Ah and S930/Ah reveal similar tendencies in mechanical properties with increased aging time. When the aging time exceeds 1 h, S870/Ah, having a large quantity of β phase, has a better vibration damping ratio than S930/Ah (containing a great quantity of primary α phase). © 2005 Springer Science + Business Media, Inc.

1. Introduction

The mechanical properties, heat treatment and damping capacity of Ti alloys have been studied and the knowledge gained has been applied to improving many processes [1–5]. Research has revealed that increases in the β content of the α/β matrix promote fracture toughness [3, 4]. However, acicular martensite can raise internal friction and thus the damping capacity of the material [6–8]. Reports also indicate that the vibration characteristics of Ti alloys are affected by microstructure [1, 2, 6–8]. Surprisingly, literature discussing Ti-Al-Mo-V alloys indicate that they possessed excellent hot workability, mechanical properties and wear resistance, but the relationship between the microstructure at near β transus temperature and vibration properties has not yet been ascertained [5, 9–11]. In the current study, the vibration damping capacity of two kinds of solid solution matrices and their aged structures will be investigated. The goal of the study of Ti-Al-Mo-V alloy is to explore the relationship between structural characteristics and vibration resistance with vibration modal analysis.

2. Experimental procedure

2.1. Materials description

The specimen used for the experiment contains 4.8 mass% Aluminum, 2.5 mass% Molybdenum and 1.4 mass% Vanadium (see Table I for detailed composition data). Fig. 1 shows the microstructures of the Ti-5Al-2.5Mo-1.4V raw material, where the darker re-

gions are β phase and the white regions are α phase. The quantitative data and mechanical properties of the raw material are given in Table II. According to previous results, the β transus of this alloy is at $\sim 900^\circ\text{C}$ [12], so the solid solution heat treatment conditions of the specimens were set at 870 and 930°C for 1 h under vacuum followed by water quenching. Hereafter, the specimens will be designated according to treatment temperature as S870 and S930. The specimens were aged at 460°C for 1–8 h and designated as S870/Axh and S930/Axh, where x represents the aging time.

The tensile mechanical properties and hardness of all specimens after heat treatment were confirmed. The dimensions of the gauge section of the tensile test specimens were 1.5 mm thick \times 4.5 mm wide \times 24 mm long and the tensile test results of each sample had a constant strain rate of $3.3 \times 10^{-3} \text{ s}^{-1}$. An image analyzer and X-ray diffraction were used for quantitative analysis of the microstructure. The Cu-K α standard ($\lambda = 1.5403 \text{ nm}$) was used for X-ray diffraction. The scanning angle was varied from 30° to 90° and the scanning velocity was $1^\circ \cdot \text{min}^{-1}$. The X-ray diffraction figures were used by integral method to measure the content of the phases. In order to understand the characteristics of the matrices, the structures of the affected regions were also observed by TEM (JEOL-JEM-3010).

2.2. Vibration modal analysis

Each specimen was fixed so that it would act as a cantilever beam. An impact hammer was used to cause

*Author to whom all correspondence should be addressed.

TABLE I Chemical composition of specimens, in mass (%)

Al	Mo	V	Fe	C	Ti
4.8	2.5	1.4	0.2	0.06	Bal.

TABLE II Quantitative structures, tensile properties and hardness of the specimens

Specimen	α (vol%)	β (vol%)	α' (vol%)	YS (kgf/mm ²)	UTS (kgf/mm ²)	EI (%)	HRC
O	62	38	–	88	91	16.1	31
S870	31	65	4	93	104	10.5	34
S930	7	–	93	102	110	4.2	36

O: raw material.

S870: solid solution treatment at 870°C for 1 h, then water quenched.

S930: solid solution treatment at 930°C for 1 h, then water quenched.

α' : martensite phase.

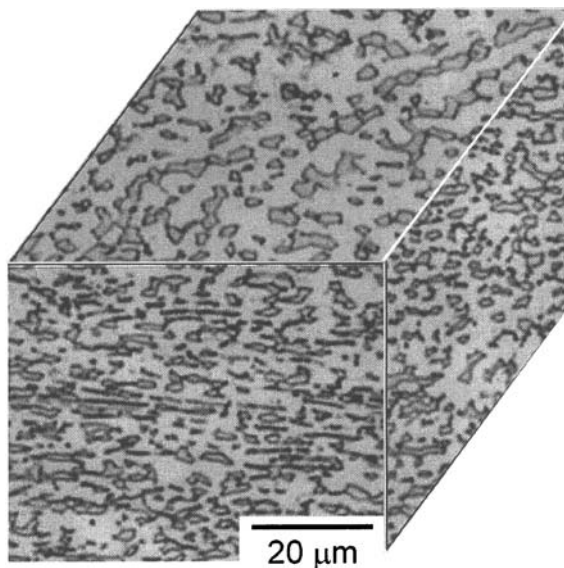


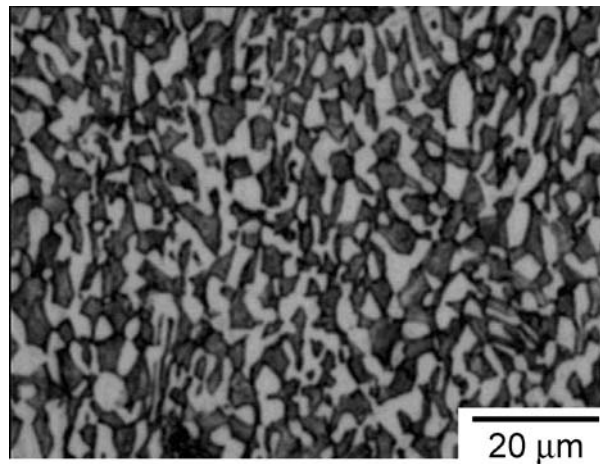
Figure 1 Optical microstructure of Ti-5Al-2.5Mo-1.4V raw material.

vibration in the beam and accelerometers were used to monitor the resulting motion. The natural frequency of the test specimens was determined from the frequency response data. The natural frequency of the specimen was selected as the standard with which to obtain the damping ratio through the half power point method [13]. The dimensions of the vibration test specimens were 1.5 mm thick \times 12 mm wide \times 90 mm long. Each vibration analysis datum was the average of at least three test results.

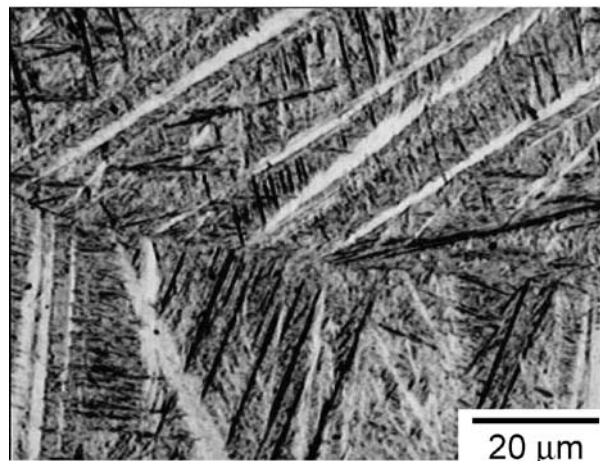
3. Results and discussion

3.1. Solid solution characteristics

The optical microstructures of S870 and S930 specimens are shown in Fig. 2. The S870 solid solution matrix has white regions (α) and dark regions (β). The S930 specimen contains needle martensite structures (α'). The TEM analyses of S870 and S930 are shown in Figs 3 and 4 respectively. Fig. 3 reveals α' in the small β region (the concentration of V and Mo were low). The S930 specimen matrix contains lath α in addition



(a)



(b)

Figure 2 Optical microstructure of solid solution specimens: (a) S870 and (b) S930.

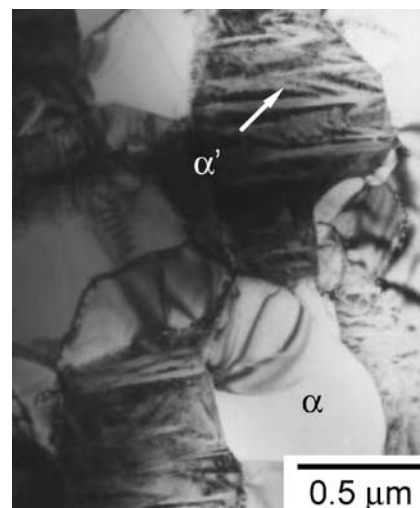


Figure 3 Transmission electron micrograph and SADP of S870.

to α' (see Fig. 4). In the current study, the solid solution matrix is divided into two systems: the $\alpha + \alpha' + \beta$ matrix (S870 specimen) and the $\alpha + \alpha'$ matrix (S930 specimen).

The quantitative data of the above structures including tensile properties and hardness data is provided in Table II. Comparing S870 with S930, increasing the α'

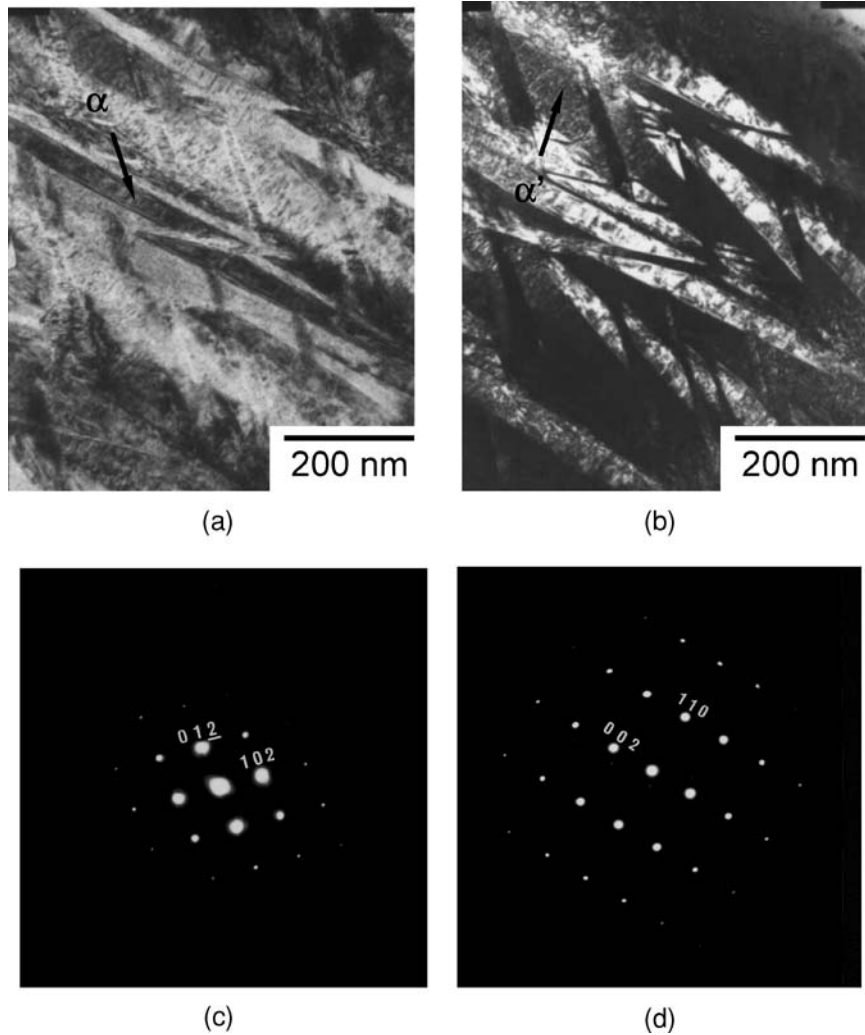


Figure 4 Transmission electron micrograph and SAED of S930: (a) BF image, (b) DF image, (c) and (d) SAED pattern of α' .

phase content improves strength and hardness but reduces ductility. Except α' phase, increasing the β content also results in changes similar to these mentioned above. In order to understand the effect of solid solution structures on vibration, the damping ratio was measured.

The damping ratios, DR, determined by the vibration modal analysis are given in Fig. 5. The S930 specimen possesses the best vibration resistance. Also, it can be seen from Fig. 5 that increasing the α' or β content can improve the damping ratio, even if the specimen has lower ductility. Most of the available literature indicates that both increasing internal friction and improving fracture toughness can increase the damping capacity of Ti alloys [3, 6–9]. For the S930 specimen, the ~ 93 vol% α' (see Table II) provides a great deal of internal friction. To give supporting evidence for this, a matrix with 100 vol% α' was obtained (it's treatment was at 1020°C for 1 h, water quenched) and designated as S1020 (not listed in Table II). The vibration damping ratio of S930 was still higher than that of S1020 (the average damping ratio of S930 is about $\sim 78 \times 10^{-4}$; S1020's is about $\sim 65 \times 10^{-4}$). This evidence also indicates that the ~ 7 vol% α -Ti of S930 (see Table II) also increases the vibration resistance. Aside from the effects of α' phase, it has also been found that

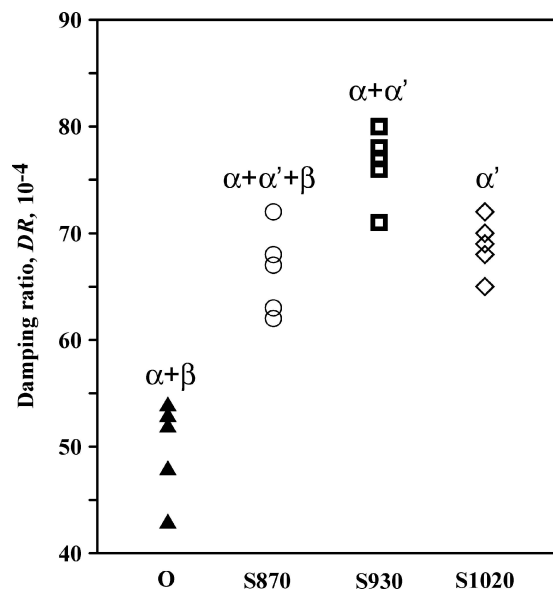


Figure 5 Damping ratio of solid solution specimens.

increasing the β content increases fracture toughness and thus vibration resistance [3, 4]. The important result is that the relationship between vibration resistance and tensile strength has been deduced for solid solution matrices.

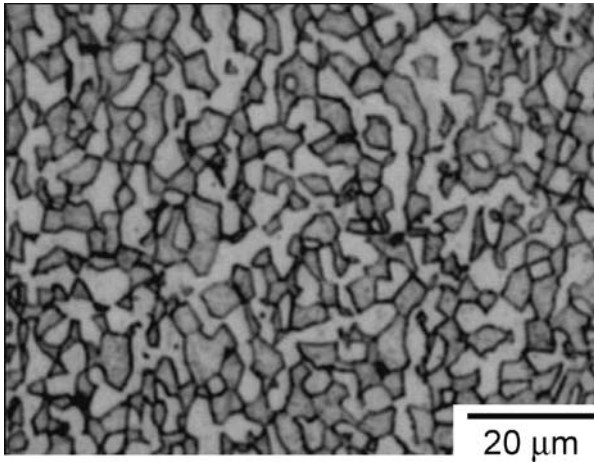


Figure 6 Microstructure of S870/A8 h specimen.

3.2. Aged characteristics

The S870 and S930 specimens that were aged at 460°C for 1–8 h are designated as S870/Axh and S930/Axh. Regardless of the aging duration, the structures of the S870/Ah specimens did not change obviously according to OM analysis. But the β phase grain size of S870/Axh specimen increased with increased the aging time. The optical microstructure of S870°C/A8h is shown in Fig. 6 (compare this with Fig. 2a). According to TEM images (see Fig. 7), the α' in the β re-

gion of the S870/A4h specimen transforms into a finer needle structure with increased aging time. However, the change in the aged structure of S930/Axh is readily apparent. For the S930/A1h specimen in Fig. 8a, many primary α phases formed along the former β grain boundaries in the martensite matrix (compare this with Fig. 2b). Prolonging the aging duration causes the grain size and the amount of primary α to increase, and the needle structure of the α' matrix apparently disappears (see Fig. 8b). Table III shows the tensile properties and hardness of the aged specimens. The mechanical properties of the S870/Axh and the S930/Axh specimens follow similar trends with increased the aging time. Except for elongation, the properties of S930/Axh have higher values than these of S870/Axh. The relationship between aging time and change in mechanical properties is roughly linear, but the change in damping is very non-linear.

The damping ratio (DR) of the aged specimens determined by the vibration modal analysis is shown in Fig. 9. For comparison, the damping ratios of the non-aged specimens (S870 and S930) are also shown in Fig. 9. For the S870/Axh, the peak of damping ratio curve occurs at the 4 h point. However, the maximum value of the damping ratio curve is observed at the 1 h point for S930/Axh. After aging for more than 2 h, the vibration resistance of S870/Axh is better than that of S930/Axh.

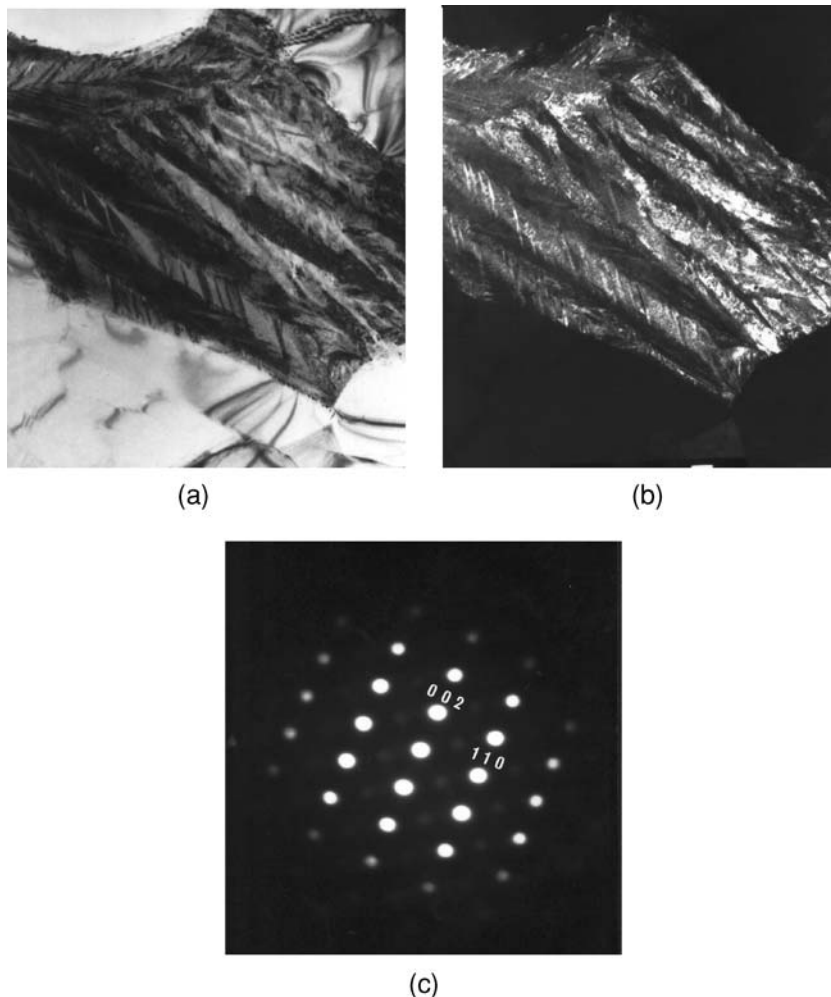
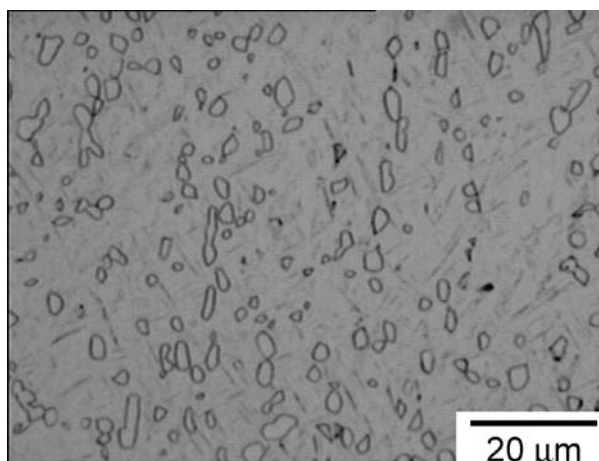
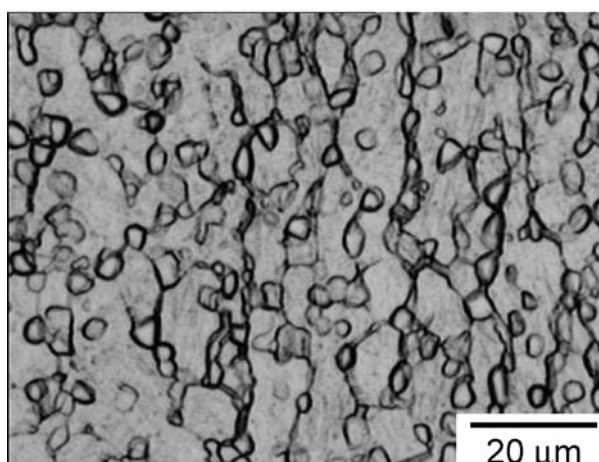


Figure 7 Transmission electron micrograph and SADP of S870/A4 h: (a) BF image, (b) DF image, and (c) SAED pattern of α' .



(a)



(b)

Figure 8 Microstructure of the aged heat treatment specimens: (a) S930/A1 h and (b) S930/A8 h.

It can be seen from Fig. 9 that after 2 h of aging, the DR of S930/Axh drops significantly below that of non-aged S930. The most likely explanation for this is that a large amount of primary α forms in the martensite matrix increasing strength and hardness but greatly reducing vibration resistance. The DR of S870/Axh aged from 1 h to 6 h is still higher than that of non-aged S870. This is because S870/Axh still possesses a large quantity of β phase and the α' phase transforms into a finer needle structure both of which promote vibration damping. The mechanism of vibration damping will be confirmed by vibration crack dissemination in a future study.

TABLE III Tensile properties and hardness of 460°C aged specimens

S870/Axh					
Aged time	1 h	2 h	4 h	6 h	8 h
YS (kgf/mm ²)	100	104	106	108	111
UTS (kgf/mm ²)	106	109	110	114	115
El (%)	6.4	6.2	5.3	4.7	4.1
HRC	37	37	38	40	40
S930/Axh					
Aged time	1 h	2 h	4 h	6 h	8 h
YS (kgf/mm ²)	105	107	111	116	117
UTS (kgf/mm ²)	112	118	119	120	122
El (%)	3.7	3.4	2.9	2.5	2.1
HRC	40	41	41	43	43

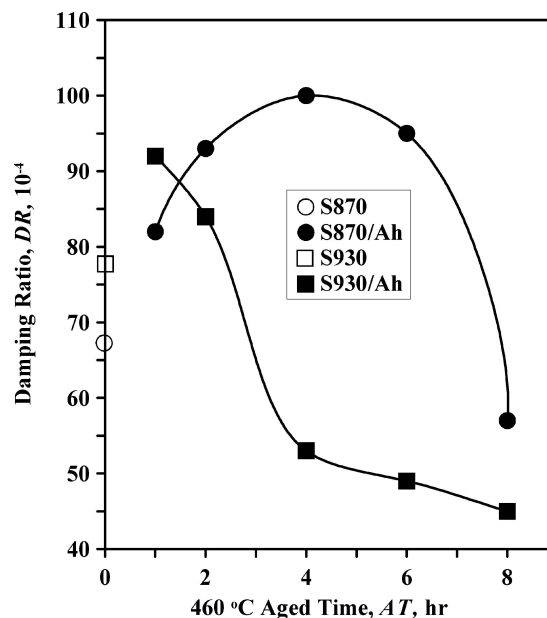


Figure 9 Damping ratio of S870/Axh and S930/Axh at 460°C aged. (The only solid solution data was shown in Y-axis)

It should be noted that the vibration resistance of the aged specimens does not seem to be significantly affected by the increased strength and hardness of the system. Additionally, the heat treatment conditions must be chosen very precisely, so as to attain desired matrix otherwise the vibration resistance cannot be improved even if the Ti alloy has better strength and hardness.

4. Conclusion

Based on the above results and discussion, the following conclusions can be drawn.

- (1) If the solid solution temperature of Ti-5Al-2.5Mo-1.4V alloy is chosen at a point above β transus, the structure contains α' (matrix)+ α and thus possesses better vibration resistance. The DR of the solid solution specimen increases with increased the strength and hardness.
- (2) The vibration resistance of the aged structure decreases as primary α phase forms in the α' matrix. After 2 or more hours of aging, the DR of the β (matrix)+ α + α' structure is higher than that of the α' (matrix)+ α structure. The vibration resistance of the aged specimen does not correlate with increased strength and hardness for this system.

Acknowledgment

The authors are grateful to the Chinese National Science Council for its financial support (Contract: NSC 93-2216-E-006-012). We are also grateful for the assistance of C. Y. Chao and B. T. Wang in obtaining materials and vibration analysis equipment.

References

1. J. E. GRADY and B. A. LERCH, NASA Lewis Research Center, SAMPE Quarterly (USA) 23(2) (1992) 11.

2. A. P. YAKOVLEV, A. U. BEREGOVENKO and V. S. LUKYANOV, *Problemy Prochnosti* **5** (1998) 71.
3. S. MUNEKI, Y. KAWABE and J. TAKAHASHI, *J. Jpn Inst. Met.* **57**(3) (1993) 268.
4. K. RUDINGER, *Z. Werkstofftech* **13**(7) (1982) 229.
5. X. S. GUAN, H. NUMAKURA, M. KOIWA, K. HASEGAWA and C. OUCHI, *Mater. Sci. Engng. A* **272**(1) (1999) 230.
6. L. A. BOCHHAROVA and V. V. MATVEEV, *Problemy Prochnosti* **5** (1973) 48.
7. Y. U. N. V'YUNENKO, B. S. KRYLOV and V. A. LIKHACHEV, *Fiz. Met. Metall.* **49**(5) (1980) 1032.
8. X. L. LU, W. CAI and L. C. ZHAO, *J. Mater. Sci. Lett.* **22**(18) (2003) 1243.
9. A. Z. PIMENOVA, A. P. TERNOVSKII and S. V. IVANOV, *Intern. J. Fatigue* **3**(4) (1981) 205.
10. A. G. KLABUKOV and A. M. ZUEV, *Mashinostroenie* **3** (1974) 120.
11. A. OGAWA, M. NIIKURA, C. OUCHI, K. MINIKAWA and M. YAMADA, *Int. J. Test. Eval.* (1996) 100.
12. H. ONODERA, Y. RO, T. YAMAGATA and M. YAMAZAKI, *Titan. Sci. Techn.* **3**(1985) 1883.
13. B. T. WANG and C. R. FULLER, *J. Chin. Soc. Mech. Engng.* **15**(1) (1994) 30.

*Received 14 September
and accepted 22 November 2004*